Friction of ice measured using lateral force microscopy

Hendrik Bluhm, Takahito Inoue,* and Miquel Salmeron†
Materials Sciences Division, Lawrence Berkeley National Laboratory, University of California, Berkeley, California 94720
(Received 16 June 1999)

The friction of nanometer thin ice films grown on mica substrates is investigated using atomic force microscopy (AFM). Friction was found to be of similar magnitude as the static friction of ice reported in macroscopic experiments. The possible existence of a lubricating film of water due to pressure melting, frictional heating, and surface premelting is discussed based on the experimental results using noncontact, contact, and lateral force microscopy. We conclude that AFM measures the dry friction of ice due to the low scan speed and the squeezing out of the water layer between the sharp AFM tip and the ice surface.

I. INTRODUCTION

Because of its importance in everyday life, the friction of ice has been investigated systematically for about a century already.[1] It is now widely accepted that a thin water layer between the slider and the ice surface causes the exceptionally low friction of ice at temperatures close to the melting point. However, the mechanism for the generation of the liquid layer was controversial in the past. Reynolds suggested in 1901 that the layer is formed by pressure melting, which is caused by the higher density of water with respect to ice.[2]

Bowden and Hughes recognized in the 1930s that the pressure melting effect in the case of skiing and skating is not sufficiently strong to cause melting of ice at temperatures below $-0.5\,^{\circ}\mathrm{C}$.[3] They performed a series of experiments that proved that the main contribution to the generation of a water layer comes from frictional heating. These results have been confirmed in many other subsequent investigations, and today frictional heating is the accepted explanation.[4,5,6,7]

A third explanation for the existence of a water film is the premelting of ice, which leads to the presence of a so-called ''liquid-like'' layer (LLL) at the surface.[8] The thickness of the LLL has been measured using various methods, and these measurements have yielded divergent results.[9] In discussions of the low friction of the ice surface, the existence and role of the LLL has been mostly neglected up to now.

For the investigation of the frictional properties of surfaces at a microscopic scale, two methods have proven to be the most effective: the surface forces apparatus[10,11] (SFA) and the atomic force microscope[12] (AFM) operated in the lateral force mode.[13] Both methods provide a single asperity contact between the surfaces in contact and thus enable us to determine the real contact area.

AFM has already been shown to be suitable for the measurement of the properties of bulk ice surfaces[14,15,16,17,18] and molecularly thin ice films.[19] In order to reliably measure the frictional properties on a microscopic scale, the surface has to be atomically flat over tens of nanometers.[20] This is difficult to achieve for polycrystalline ice surfaces with their unknown local surface orientation. Even for single crystalline ice, the high dynamic nature of the surface at temperatures close to the melting point (rate of evaporation and condensation) leads to faceting and fluctuations in the surface topography.[21]

As we have shown in a previous paper,[19] thin ice films (thickness<3 nm) grown on a mica substrate are remarkably smooth (atomically flat over micrometers) and possess a stable morphology as long as the thermodynamic conditions in the experiment are kept constant. These surfaces are therefore promising candidates for the study of the friction of ice using AFM.

In addition to providing a well-defined contact area between tip and surface, the AFM technique is also well suited for the investigation of the three explanations for the existence of a liquid layer at the interface between tip and ice. Since the contact area can be calculated from the known parameters of the system—tip radius, normal force, and elastic properties of tip and ice—the *pressure melting* effect can be measured. The effect of *frictional heating* can be determined from the known contact area, scanning speed and thermal conductivity of the materials in contact during scanning. Finally, the role of *surface premelting* can be investigated due to the ability of AFM to operate both in contact and non-contact modes. The thickness and distribution of the LLL on the ice surface can in fact be mapped by operating the AFM in the noncontact scanning polarization force microscopy mode (SPFM),[22] as we have shown in a previous paper.[19]

Here we will describe AFM investigations on the friction of ice performed on molecularly thin ice films grown on mica substrates. We will compare our results with those obtained in previous experiments using macroscopic methods.

II. EXPERIMENT

The experiments were performed using a homebuilt AFM housed in a vacuum chamber. The experimental setup has been described in a previous paper.[23] The ice films were grown on mica substrates cleaved *in situ*. The experiments were carried out in the temperature range from -24 to $-40\,^{\circ}\mathrm{C}$. Distilled water with a specific resistivity of 18.2 $\mathrm{M}\Omega\,\mathrm{cm}$ was used as source for the water vapor. The water was purified in three successive pump-freeze cycles. The water vapor pressure in the chamber was measured with an accuracy of 0.02 torr using a capacitance sensor pressure gauge.

At the beginning of the experiments, the chamber was evacuated to its base pressure ($\sim 10^{-6}$ torr). Afterwards, water vapor ($p < 0.5$ torr) was introduced into the chamber, and the sample was cooled. While cooling, the sample was kept undersaturated with respect to the vapor pressure in order to avoid macroscopic ice growth. At a given fixed vapor pressure (in the range from 0.5 to 0.1 torr for temperatures of -24 to $-40\,^{\circ}$C, respectively), the sample temperature was briefly decreased to oversaturation values with respect to the vapor, thus initiating ice growth on the substrate. Then the sample temperature was increased again to a value that corresponds to 85% relative humidity (RH) at the given water vapor pressure. At this RH value, ice films with a thickness of several bilayers are stable on the mica surface.[19]

Our AFM is controlled by commercial feedback electronics.[24] Triangularly shaped silicon cantilevers with a spring constant of 0.4 N/m were used.[25] These are boron-doped and have a resistivity of $10^{-3}\,\Omega$ cm, which is sufficient for use in SPFM measurements. SPFM images were taken with a tip-to-sample distance of $\sim$40 nm and at a tip-to-sample bias of ± 5 V. Details of SPFM imaging of ice are described in Ref. 19.

Care has to be taken in the experiments to exclude any damage of the ice films due to possible temperature differences between the tip and the surface. We have estimated the tip temperature by employing the bimorph properties of the cantilever (silicon body with gold coating). The bending of the cantilever when it is in close proximity of the cold sample surface provides a measure for its temperature. At a tip-to-sample distance of 20 nm and at a sample temperature of $-20\,^{\circ}$C, the tip temperature was estimated to be $-15\,^{\circ}$C. The tip temperature will be even closer to that of the sample when the tip is in contact. We also left the tip in contact with the ice surface for as much as half an hour without observing any changes in the surface morphology. Therefore damage of the sample surface due to heating by the tip is highly unlikely. Details of the measurement of the cantilever temperature can be found in Ref. 19.

In the contact operation mode of the microscope, the cantilever bending (normal force) and twisting (lateral force) were measured simultaneously. Normal forces were calculated from the known normal spring constant of the cantilever. Values for the lateral deflection of the cantilever (as a consequence of the lateral force acting on the tip) were obtained according to a standard procedure described in Ref. 26. These values were then converted into a friction force using a lateral spring constant, which was calculated from the known dimensions of the cantilevers.[27]

The normal force in the contact images varied in the range from 10 nN to 350 nN for pressure-melting experiments. Typical scan speeds were ~ 5 μm/s. The radius of the tip used in our experiments was 200 nm, as determined using a $SrTiO_3$ grating.[28,29]

III. RESULTS AND DISCUSSION

A. Structure and properties of the ice films

Figure 1(a) shows an SPFM (noncontact) image that was taken after a thin ice layer was grown on the mica substrate in the way described in Sec. II. The sample temperature is $-24\,^{\circ}$C, and the relative humidity 85%. The surface is covered with droplets, which have a maximum height of 15 nm and a maximum diameter of 1.5 μm at the base. Figure 1(b) shows a topographical image acquired in contact mode with a normal force of 30 nN at the same location, just after acquisition of the SPFM image. The pressure and temperature are the same as in Fig. 1(a). Large, flat ice platelets with a height of 2 to 3 nm relative to the substrate can be seen.

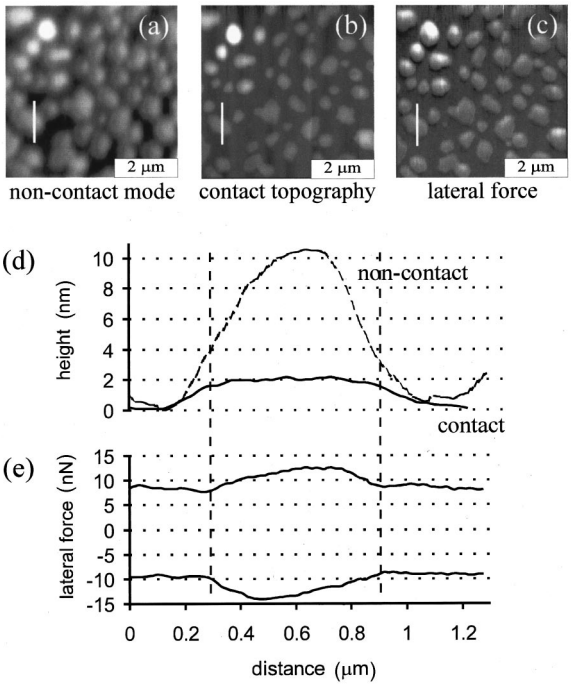

FIG. 1. (a) Noncontact SPFM image taken after condensation of water on the mica substrate following a brief temperature excursion to supersaturation conditions. The image was taken at $T_{\text{sample}} = -24\,^{\circ}$C and a relative humidity of 85%. The maximum height of the droplets is 15 nm and the maximum diameter at their base 1.5 μm. (b) Contact mode image acquired at the same location as in (a) after the SPFM image was taken. Flat ice platelets are observed with a height of 2 to 3 nm relative to the substrate. The platelets are positioned at the same locations as the droplets shown in (a). (c) Lateral force image taken simultaneously with the contact mode image. A brighter contrast means a higher lateral force. The lateral force is highest on the ice platelets. (d) Comparison of cross sections along the lines indicated in (a) and (b). The droplet is sitting on an ice platelet. From the height difference between SPFM and contact mode images, the thickness of the liquid layer is estimated to be 8 nm. (e) Friction loop taken along the line indicated in (c), i.e., at the same position as the cross sections for the topographical images. The width of the friction loop is a measure for the lateral force. The lateral force is higher on ice than on mica.

A comparison of the images in Figs. 1(a) and 1(b) indicates that the position of the ice platelets coincides with that of the droplets imaged using noncontact SPFM. In Fig. 1(d) cross sections along the lines shown in Figs. 1(a) and 1(b) are given. While the height of the droplet in the SPFM image is 10 nm, the measured height in contact is only 2 nm. This points to the existence of a liquid layer with a thickness of 8 nm, covering the ice platelet.[30] The liquid nature of the droplets is supported by the increased adhesion observed in the approach part of force vs distance curves, as compared to areas that are not covered by the droplets.

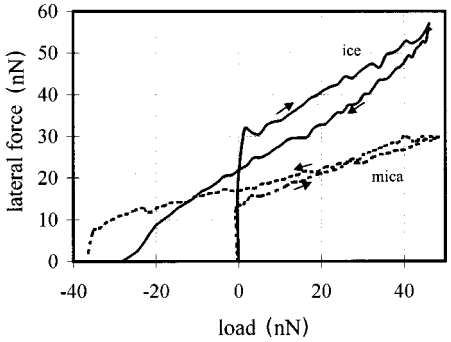

FIG. 2. Lateral vs normal force curves for ice, at $T=-24\,^{\circ}\mathrm{C}$ (solid line), and for mica, at room temperature (dashed line). Arrows mark the curves for increasing and decreasing load. From the slopes of the linear portion of the curves, a ''friction coefficient'' for ice (0.6) and mica (0.3) can be obtained. The curves were taken using a triangularly shaped silicon cantilever with a normal spring constant of 0.4 N/m.

B. Frictional properties of ice films

A lateral force image acquired simultaneously with the contact topography image is presented in Fig. 1(c). A brighter contrast means a higher lateral force. The tip experiences a higher lateral force on the ice platelets than it does on the mica substrate. The friction force measured in the forward and backward directions (i.e., the ''friction loop'' [20]) on the platelet for which cross sections are given in Fig. 1(d) is shown in Fig. 1(e). The width of the friction loop is a measure for the lateral force. The friction loop is wider for ice than for mica.

After taking this measurement, we performed lateral force vs load measurements on ice. A flat ice island was chosen, and the lateral force was measured as a function of normal force, according to the method described in Ref. 26. The result is shown in Fig. 2. The lateral force is shown for both increasing and decreasing normal force (see arrows in Fig. 2). The adhesion between tip and surface is 25 nN, as can be deduced from the retracting curve. For comparison, a similar lateral force vs load measurement corresponding to mica at room temperature and 30% RH is shown. From these curves we can determine a ''friction coefficient'' for both ice and mica. The term ''friction coefficient'' has to be used with care in this case, since Amontons's law (lateral force F_L equals normal force F_N times friction coefficient μ[31]) is not valid for single asperity contacts at low loads. In that case, the lateral force is proportional to the contact area and the shear strength of the junction between tip and surface.[32] However, in order to compare our results to those from macroscopic measurements, we will use the slope of the nearly linear part of the curves in Fig. 2 as a measure of the friction coefficient. The values found are 0.6 for ice, and 0.3 for mica.

The curves shown in Fig. 2 are representative of all the measurements that we carried out in the temperature region from -24 to $-40\,^{\circ}\mathrm{C}$. Ice always showed a higher friction than mica, in apparent contradiction with our everyday experience. The friction coefficient of ice was on the order of 0.6 in the entire temperature region. This value is in the range of the static friction coefficient measured in macroscopic experiments.[33] This seems to indicate that there is no lubricating water layer between the tip and the ice surface. In the following, we present additional results and a more detailed discussion in regard to the three possible mechanisms for the generation of a water film at the ice surface.

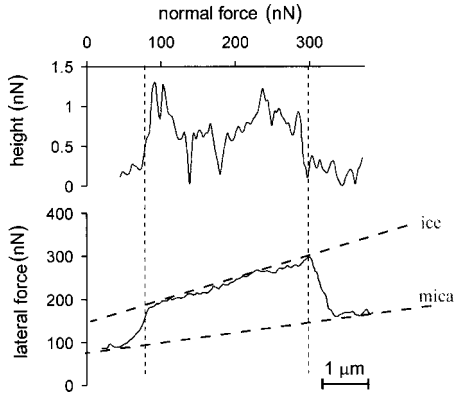

FIG. 3. (a) Topographic profile acquired while increasing the normal force from left to right over an ice island at $T=-24\,^{\circ}\mathrm{C}$. The height of the island remains approximately constant over the range of normal forces, showing that it can sustain the pressure exerted by the tip. (b) Lateral force vs normal force profile acquired while increasing the load. The curve was obtained simultaneously to the topography data shown in (a). The slopes of the lateral force vs normal force values on mica and ice, respectively, confirm the data shown in Fig. 2.

C. Pressure melting

The pressure melting effect can be investigated in a similar fashion as described for the compression of self-assembled monolayer islands in Ref. 34. To this end, the tip is scanned over an ice island at progressively higher loads. At the same time, the height of the island is measured. If pressure melting occurs, the height should decrease with load. No such decrease was observed.

On theoretical grounds, pressure melting is not expected either, since at temperatures below $-22\,^{\circ}\mathrm{C}$ there is no liquid phase in the phase diagram of water.[35] Instead, at sufficiently high pressure, a phase transition ice Ih→ice III (for $T=-24$ to $-35\,^{\circ}\mathrm{C}$), or ice Ih→ice II (for $T=-35$ to $-40\,^{\circ}\mathrm{C}$) is possible.[1] The threshold pressure for the transition ice Ih→ice III is 2.08×10^{8} MPa. This corresponds to a normal force of 180 nN for our tip radius of 200 nm (calculated using the Hertz model[36]). The corresponding values for the transition ice Ih→ice II are 2.13×10^{8} MPa, and 200 nN, respectively.

To investigate the possibility of tip-induced phase transitions, we subjected the ice islands to a load of up to 350 nN. The experiment was performed at $T=-24\,^{\circ}\mathrm{C}$. The normal force was increased while scanning over an ice island. A cross section of the island topography along the scanning direction is given in Fig. 3(a). Although the image becomes increasingly noisy due to the high normal forces, the height of the island remains constant (0.8 nm) over the whole normal force range up to the highest normal force of 290 nN. This proves that the ice islands can sustain the pressure exerted by the tip.

The lateral force measured simultaneously along the topographic profile is shown in Fig. 3(b). A phase transition

could lead to a jump in the lateral force, since the friction is sensitive not only to the chemical composition of a surface but also to its crystallographic properties.[37] However, no discontinuities were observed in the lateral vs normal force curve. These results indicate that pressure induced melting or phase transitions do not play a significant role in the friction properties of the nanometer thin ice islands presented here.

D. Frictional heating

The effect of frictional heating can be estimated from the known contact area, scanning speed, and thermal conductivity of the materials in contact during scanning. We follow the method described by Oksanen and Keinonen in Ref. 6. Three energy terms are important. One is the amount of heat necessary to melt a layer of ice of thickness z at the interface between tip and slider (Q_M). The second is the heat produced by friction (Q_F). Finally we need to determine the amount of heat conducted away from the interface into the tip, as well as into the ice film and mica substrate (Q_C). Melting occurs when $Q_M < Q_F - Q_C$. The frictional heating depends critically on the scanning speed. The thickness z of the melted layer on the ice surface as a function of speed can be calculated according to Eq. (11) in Ref. 6:

$$z(\nu) = \frac{1}{h_{\text{water}}\rho_{\text{water}}}\left[\frac{\mu F_N}{D} - \Delta T\left(\frac{D}{2\nu}\right)^{1/2}(\lambda_{\text{mica}} c_{\text{mica}} \rho_{\text{mica}})^{1/2}\right]. \tag{1}$$

We used the following values for the parameters: normal force, $F_N = 30\,\text{nN}$; tip radius, 200 nm (yielding a contact diameter of $D = 18\,\text{nm}$); friction coefficient, $\mu = 0.6$; latent heat of water, $h_{\text{water}} = 2.4\times10^5\,\text{J kg}^{-1}$; density of water $\rho_{\text{water}} = 10^3\,\text{kg m}^{-3}$; heat conductivity of mica,[38] $\lambda_{\text{mica}} = 0.7\,\text{W m}^{-1}\,\text{K}^{-1}$; heat capacity of mica,[39] $c_{\text{mica}} = 502\,\text{J kg}^{-1}\,\text{K}^{-1}$; and density of mica,[38] $\rho_{\text{mica}} = 2800\,\text{kg m}^{-3}$. In Eq. (1), we have neglected the conduction of heat into the tip, since this is only a minor contribution compared to the heat conduction into the substrate. We have also assumed that the ice layer has no significant influence on the heat conductivity into the substrate due to its thickness of only a few monolayers. Since the temperature of the melted layer at the ice surface is by definition 0 °C, the temperature difference ΔT between substrate and surface in the case of melting is 24 °C for our case.

Using Eq. (1), we calculated the thickness z of the melted layer as a function of the scanning speed. We find that, for speeds below 4 m/s, no melting occurs, because the amount of heat produced at the interface (Q_F) is smaller than the amount of heat conducted away from it. At a speed of 4 m/s, frictional melting sets in. With increasing speed, the thickness of the melted layer increases. These velocities are, however, orders of magnitude larger than the usual speeds in AFM experiments, which are on the order of micrometers per second. Therefore, frictional heating, which is the major contribution to the generation of a liquid layer in macroscopic skiing and skating, is not a factor in our experiments.

E. Liquidlike layer

We have shown that neither pressure melting nor frictional heating can produce a liquid layer on the surface of our ice islands. However, the images presented in Fig. 1 indicate that there is a liquid layer on the ice islands, even without the interaction of the tip with the sample. The thickness of this layer was determined to be ~8 nm. Despite this, the lateral force on ice is not reduced and is on the same order as the static friction in macroscopic experiments, as we concluded from Fig. 2. Therefore we must check whether some of this liquid remained trapped between the tip and the ice surface or if the tip completely penetrated the liquid layer.

One method to calculate the penetration depth of the tip is to use considerations of fluid mechanics.[40] When a probe is in contact with a lubricating film on a solid substrate, some of the lubricant is squeezed out of the junction due to the pressure exerted by the probe. The thickness z of the layer that remained between the probe and the substrate can be calculated as a function of time t according to

$$\frac{1}{z^2(t)} - \frac{1}{z_0^2} = \frac{16\,t\sigma_0}{3\,\eta_{\text{water}} D^2}, \tag{2}$$

where σ_0 is the pressure at the junction between slider and surface, η the viscosity of the lubricant, D the contact diameter, and z_0 the initial thickness of the lubricant.[40] Keeping in mind that continuum theory is not strictly valid for molecularly thin lubricating films,[40] we can obtain and estimate the thickness of the water layer trapped under the tip in our experiment. Let us assume the same experimental conditions as in Sec. II D, i.e., $D = 18\,\text{nm}$; $\sigma_0 = 10^8\,\text{N m}^{-2}$ (for $F_N = 30\,\text{nN}$); viscosity of water[38] $\eta_{\text{water}} = 1.8\times10^{-3}\,\text{N s m}^{-2}$ (at 0 °C); initial height of the water layer $z_0 = 8$ nm (according to Fig. 1). From Eq. (2), we obtain that it takes less than only 10^{-6} s to reduce the initial water layer thickness of 8 nm between the tip and the ice islands to less than 2 Å. We can estimate a characteristic time interval for the interaction of the tip with the sample considering the scan speed (5 $\mu\text{m s}^{-1}$) and the contact diameter. This interaction time is in the range of milliseconds, i.e., orders of magnitude longer than it takes to squeeze out the water layer between the tip and surface. The lubricating water film between the ice and tip would therefore have a significant thickness only at scan velocities higher than millimeters per second.

Another effect that could play a role is the solidification of the fluid film when it is confined to a thickness of only a few monolayers between two surfaces.[40] For a thick film (more than about 10 monolayers), the yield stress (the tangential stress to initiate sliding of the two surfaces relative to each other) is usually very small, but for thinner films a finite yield stress is observed.[40,41] This increased yield stress would also lead to a higher lateral force.

From the above discussion, we conclude that in our AFM experiments we measured the ''dry friction'' of ice. This friction is higher than that of mica. This could be caused by different energy dissipation processes taking place in these two different surfaces. The breaking of hydrogen bonds, for instance, could be a major factor for the loss of energy during friction on ice, whereas the stronger covalent bonds of the silicon oxide tetrahedra at the mica surface are less likely to be destroyed. While for mica the contribution of atomic scale wear can be observed at sufficiently high load, *via* changes in the surface topography,[42] the same is difficult to

achieve for the surface of ice. Since our ice films are in thermodynamic equilibrium with their vapor with fast molecular exchange rates, an instantaneous ''healing'' of such defects would prevent their observation.

The main difference of our experiments compared to conventional measurements under macroscopic conditions is the extremely low scan speeds and the small contact area between the tip and surface. So while our experiments might not be significant for the understanding of such phenomena as skiing and skating, they might be relevant to the friction properties of surfaces covered by thin ice films formed in slight undersaturation conditions.

The mechanical and thermodynamic stability of the ice islands grown on mica substrates, and their smoothness, presents us with the opportunity to investigate the friction on ice on the molecular scale. These investigations are under way in our laboratory.

IV. SUMMARY

We have investigated the friction of nanometer-thin ice islands using combined non-contact (SPFM), contact topography, and lateral force operation modes of the AFM. A friction coefficient of 0.6 was measured for ice in the temperature range from -24 to $-40\,^{\circ}\mathrm{C}$. This value is comparable to the static friction measured in macroscopic experiments. The high friction is due to the absence of a lubricating water layer between tip and surface, i.e., the AFM measures dry friction under our experimental conditions. It was found that pressure melting and frictional heating did not play a significant role in our experiments. A liquid-like layer with a thickness of 8 nm is present over the ice surface under our conditions. This layer did not contribute to the lubrication of the contact between the tip and ice surface, because it is squeezed out due to the small contact area and the low scan speed (micrometers per second).

ACKNOWLEDGMENTS

This work was supported by the Director, Office of Science, Office of Basic Energy Sciences, of the U.S. Department of Energy under Contract No. DE-AC03-76SF00098. The authors thank D.F. Ogletree for helpful discussions. H. Bluhm acknowledges support from the Alexander von Humboldt Foundation, Bonn, Germany.

*Present address: Electrotechnical Laboratory, Ministry of International Trade and Industry, 1-1-4 Umezono, Tsukuba, Ibaraki 305, Japan. Electronic address: tinoue@etl.go.jp

†Author to whom correspondence should be addressed. Electronic address: salmeron@stm.lbl.gov

[1] For a review, see P. V. Hobbs, *Ice Physics* (Clarendon Press, Oxford, 1974), pp. 411–421.

[2] O. Reynolds, *Papers on Mechanical and Physical Subjects* (Cambridge University Press, Cambridge, England, 1901), Vol. 2, pp. 734–738.

[3] F. P. Bowden and T. P. Hughes, Proc. R. Soc. Math. Phys. Sci. **172**, 280 (1939).

[4] D. C. B. Evans, J. F. Nye, and K. J. Cheeseman, Proc. R. Soc. London, Ser. A **347**, 493 (1976).

[5] M. Akkok, C. M. McC. Ettles, and S. J. Calabrese, J. Tribol. **109**, 552 (1987).

[6] P. Oksanen and J. Keinonen, Wear **78**, 315 (1982).

[7] S. C. Colbeck, Am. J. Phys. **63**, 888 (1995).

[8] For a review on premelting of ice, see J. G. Dash, H. Fu, and S. Wettlaufer, Rep. Prog. Phys. **58**, 115 (1995).

[9] A comparison of the results obtained with different methods is given in Fig. 1 of M. Elbaum, S. G. Lipson, and J. G. Dash, J. Cryst. Growth **129**, 491 (1993).

[10] J. N. Israelachvili, P. M. McGuiggan, and A. M. Homola, Science **240**, 189 (1988).

[11] J. Peachey, J. Van Alsten, and S. Granick, Rev. Sci. Instrum. **62**, 463 (1991).

[12] G. Binnig, Ch. Gerber, and C. F. Quate, Phys. Rev. Lett. **56**, 930 (1986).

[13] C. M. Mate, G. M. McClelland, R. Erlandsson, and S. Chiang, Phys. Rev. Lett. **59**, 1942 (1987).

[14] O. Nickolayev and V. F. Petrenko, in *Evolution of Thin Film and Surface Structure and Morphology*, edited by B. G. Demczyk, MRS Symposia Proceedings No. 355 (Materials Research Society, Pittsburgh, 1995), p. 221.

[15] V. F. Petrenko, J. Phys. Chem. B **101**, 6276 (1997).

[16] C. R. Slaughterbeck, E. W. Kukes, B. Pittenger, D. J. Cook, P. C. Williams, V. L. Eden, and S. C. Fain, J. Vac. Sci. Technol. A **14**, 1213 (1996).

[17] B. Pittenger, D. J. Cook, C. R. Slaughterbeck, and S. C. Fain, J. Vac. Sci. Technol. A **16**, 1832 (1998).

[18] A. Doeppenschmidt, M. Kappl, and H.-J. Butt, J. Phys. Chem. B **102**, 7813 (1998).

[19] H. Bluhm and M. Salmeron, J. Chem. Phys. **111**, 6947 (1999).

[20] For a review on lateral force microscopy, see, for example, R. W. Carpick and M. Salmeron, Chem. Rev. **97**, 1163 (1998).

[21] H. Dosch, A. Lied, and J. H. Bilgram, Surf. Sci. **327**, 145 (1995).

[22] J. Hu, X.-D. Xiao, and M. Salmeron, Appl. Phys. Lett. **67**, 476 (1995); J. Hu, X.-D. Xiao, D. F. Ogletree, and M. Salmeron, Science **268**, 277 (1995).

[23] H. Bluhm, S. H. Pan, L. Xu, T. Inoue, D. F. Ogletree, and M. Salmeron, Rev. Sci. Instrum. **69**, 1781 (1998).

[24] STM 100, RHK Technology, Rochester Hills, MI.

[25] Ultralevers, Park Scientific Instruments, Sunnyvale, CA.

[26] A. Lio, C. Morant, D. F. Ogletree, and M. Salmeron, J. Phys. Chem. B **101**, 4767 (1997).

[27] D. F. Ogletree, R. W. Carpick, and M. Salmeron, Rev. Sci. Instrum. **67**, 3298 (1996). The conversion from lateral deflection to lateral force is connected with a possible error of a factor of 2.

[28] S. S. Sheiko, M. Moeller, E. M. C. M. Reuvenkamp, and H. W. Zandbergen, Ultramicroscopy **53**, 371 (1994).

[29] R. W. Carpick, N. Agraït, D. F. Ogletree, and M. Salmeron, J. Vac. Sci. Technol. B **14**, 1289 (1996).

[30] The influence of the electrostatic interaction between the tip and the sample on the heights measured in SPFM mode is discussed in Ref. 19.

[31] G. Amontons, Histoire de l' Académie Royale des Sciences arec les Mémoires de Mathématique et de Physique, Année 1699–1708 (Amsterdam: Chez Gerald Kuyper, 1706–1709), p. 206.

[32] F. P. Bowden and D. Tabor, *Friction and Lubrication of Solids, Part II* (Clarendon, Oxford, 1964).

[33] F. P. Bowden and D. Tabor, *Friction and Lubrication of Solids, Part I* (Clarendon, Oxford, 1954), p. 68.

[34] E. Barrena, S. Kopta, D. F. Ogletree, D. H. Charych, and M. Salmeron, Phys. Rev. Lett. **82**, 2880 (1999).

[35] W. Wagner, A. Saul, and A. Pruss, J. Phys. Chem. Ref. Data **23**, 515 (1994).

[36] H. Hertz, J. Reine Angew. Math. **92**, 156 (1881).

[37] H. Bluhm, U. D. Schwarz, K.-P. Meyer, and R. Wiesendanger, Appl. Phys. A: Mater. Sci. Process. **61A**, 525 (1995).

[38] *CRC Handbook of Chemistry and Physics*, 77th ed. (CRC, Boca Raton, 1996).

[39] *CRC Handbook of Tables for Applied Engineering Science*, 2nd ed. (CRC, Boca Raton, 1976).

[40] B. N. J. Persson, *Sliding Friction, Physical Principles and Applications* (Springer, New York, 1998), pp. 115–122.

[41] M. L. Lee, P. M. McGuiggan, and J. N. Israelachvili, J. Chem. Phys. **93**, 1895 (1990).

[42] J. Hu, X.-d. Xiao, D. F. Ogletree, and M. Salmeron, Surf. Sci. **327**, 358 (1995).